



perimeter scholars  
INTERNATIONAL™



PERIMETER  
INSTITUTE  
FOR THEORETICAL PHYSICS

# Minimal Surfaces for Scattering Amplitudes and the Harmonic Oscillator

Author: Henrik P. A. Gustafsson

Supervisor: Pedro Vieira

June 1, 2012

## **Abstract**

As a first step towards calculating minimal surfaces in  $\text{AdS}_3$ , related to scattering amplitudes through the AdS/CFT correspondence, we develop a method for finding the small solutions to the Schrödinger equation written in a two-component form. The solutions are found iteratively from an integral equation resembling that of the  $Y$ -functions that previously have been used to find the minimal area. We apply our methods to the harmonic oscillator and find complete agreement with the known solutions.

# Contents

<b>1</b>	<b>Introduction</b>	<b>1</b>
<b>2</b>	<b>Background</b>	<b>2</b>
2.1	AdS/CFT correspondence . . . . .	2
2.2	Scattering amplitudes and null polygonal Wilson loops . . . . .	3
<b>3</b>	<b>Y-system</b>	<b>5</b>
3.1	Small solutions and Stokes' phenomenon . . . . .	7
3.1.1	Shift relations . . . . .	9
3.2	The Schouten identity . . . . .	9
3.3	Hirota equations . . . . .	10
3.4	Y-system equations . . . . .	11
3.5	Geometrical interpretation . . . . .	12
3.5.1	WKB limit . . . . .	12
3.5.2	Branch cuts . . . . .	14
3.5.3	Harmonic oscillator and octagon . . . . .	15
3.6	Y-system integral equations . . . . .	17
<b>4</b>	<b>Finding the small solutions</b>	<b>19</b>
4.1	Normalization . . . . .	20
4.2	Integral equation for $T_1$ . . . . .	21
4.2.1	Picking up residues . . . . .	22
4.3	Integral equation for the small solutions . . . . .	24
4.3.1	Other sectors . . . . .	26
<b>5</b>	<b>The harmonic oscillator</b>	<b>30</b>
<b>6</b>	<b>Scattering amplitudes</b>	<b>35</b>
<b>7</b>	<b>Conclusions</b>	<b>35</b>
<b>A</b>	<b>Explicit expressions</b>	<b>37</b>

# 1 Introduction

In this essay we study minimal surfaces in  $\text{AdS}_3$  that, on the boundary, end on null polygon loops as illustrated in figure 1. We seek to develop a method to iteratively find the shape of these surfaces using the  $Y$ -system formalism.

Previous work, [1], have been able to compute the area of the surfaces without knowing their shapes and we will now build upon that theory to find the actual configurations. Our approach is to first study a similar problem with known explicit solutions, namely the Schrödinger equation written in a two-component form and especially the case of the harmonic oscillator.

We derive the  $Y$ -system equations with the Schrödinger problem in mind and find an integral equation for the small solutions that, in the scattering amplitude picture, would give us the minimal surface.

After finding the surface one could start calculating corrections to the scattering amplitudes by considering fluctuations around the classical shape. We would also be able to study the surface's dependence on the polygon and investigate possible transitions. Additionally,  $Y$ -systems are encountered in a wide variety of problems where it would be useful to find the small solutions.

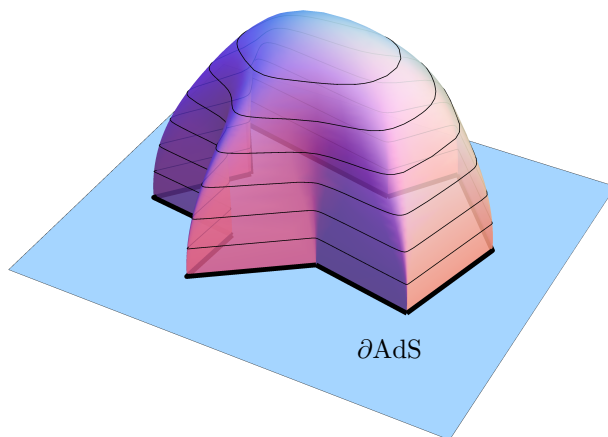


**Figure 1:** Imagined minimal surface in AdS used to calculate scattering amplitudes in  $\mathcal{N} = 4$  SYM.

This essay is organized as follows. In section two we review the background that leads to the correspondence between scattering amplitudes and minimal areas. The following section introduces the two-component formalism for the Schrödinger equation and then derives the  $Y$ -system functional relations together with their integral equations. The next section is dedicated to developing similar integral equations for the small solutions. In section five we apply our theory to the harmonic oscillator and compare our results with the known, explicit solutions. We conclude by stating how the methods can be generalized to find the minimal surfaces.

## 2 Background

Let us first introduce the background that motivates why scattering amplitudes can be calculated by finding the minimal area of a string world sheet in AdS.

### 2.1 AdS/CFT correspondence

The AdS/CFT correspondence is a conjecture that relates certain conformal field theories with certain string theories in a background with AdS (Anti-de-Sitter) as a factor. The conformal theory is living on the boundary of AdS which is conformally flat [2].

A well studied example of the conjectured duality is the conformal theory  $\mathcal{N} = 4$  SYM and type IIB string theory in  $\text{AdS}_5 \times S^5$ . Using various methods of integrability one has been able to check the correspondence in many cases and found complete agreement [2].

For the  $\mathcal{N} = 4$  SYM theory we have two important parameters:  $g_{\text{YM}}$  which is the coupling constant of the Yang-Mills theory and the rank  $N$  which states the gauge fields' symmetry group,  $SU(N)$ . It is useful to instead consider the pair  $\lambda$  and  $N$  where the former is called the 't Hooft coupling and is defined as  $\lambda = g_{\text{YM}}^2 N$ .

On the CFT side, physical quantities are usually most easily calculated by expanding in small  $\lambda$ , i.e. perturbative gauge theory, while the string theory on the AdS side is easier to understand for large  $\lambda$  where the strings become classical. Taking the so called planar limit  $N \rightarrow \infty$  while keeping

$\lambda$  fixed results in free strings as in a string coupling constant that goes to zero. All this is very beautifully explained in [2, figure 2] and surrounding text.

One important aspect of the dictionary between the two types of theories is the relation between the expectation values of Wilson loops in the CFT along a contour  $\mathcal{C}$  and the proper world sheet area of a fundamental string ending on the same contour  $\mathcal{C}$  on the boundary of AdS [3]. Beyond the classical limit  $\lambda \rightarrow \infty$  one should consider the full partition function.

## 2.2 Scattering amplitudes and null polygonal Wilson loops

Other important quantities of the conformal theory are regularized scattering amplitudes that in the strong coupling limit have been shown to be related to the area of minimal surfaces ending on polygons with light-like or null edges [4]. These edges correspond to the momenta of the massless gauge particles which forms a closed polygon because of momentum conservation.

The area of a surface ending on this null polygonal contour computes a Wilson loop. Hence, at strong coupling we have that scattering amplitudes are given by null polygonal Wilson loops. This led to the conjecture of a duality between the two at all couplings [4] which now is a statement purely on the CFT side.

In [5], Alday and Maldacena calculated the leading order contribution to the regularized four point scattering amplitude at large  $\lambda$  by finding the classical world sheet area in AdS<sub>5</sub> that ends on a polygon with four null edges.

A few years later, Alday, Maldacena, Sever and Vieira in [1] found a way to compute the area for a general number of null edges. They used methods of integrability to write a set of functional equations on the form of the Thermodynamic Bethe Ansatz equations and showed that the area is the TBA free energy.

The functional equations called the  $Y$ -system could be solved iteratively after rewriting them as integral equations. This made it possible to then find the free energy by numerical integration and thus also the area without actually finding the shape of the minimal surface. In this essay we will study similar functional equations that can be used to find the shape as pictured in figure 1.

For simplicity, we will consider minimal surfaces that can be embedded in  $\text{AdS}_3 \subset \text{AdS}_5$  for which the null polygon edges lie in a two dimensional plane. To be able to verify our methods we apply them to a problem of similar structure with known explicit solutions. It can be shown that the Schrödinger equation, rewritten in a particular way strongly resembles the initial equations of [1] for the case of  $\text{AdS}_3$ . Finding the wave function of the harmonic oscillator in this formalism is closely related to finding the minimal surface that ends on a null-edged octagon.

In fact, the two problems are so similar that we will use the more well known Schrödinger problem as a foundation for reviewing the theory behind [1]. Where differences arise we will try to diligently point them out. Let us first though, briefly present the starting point for the  $\text{AdS}_3$  picture in [1].

The integrability of the classical string model in  $\text{AdS}_5$  is closely related to the existence of a one parameter family of flat connections [1, 6]. The equations of motion for the classical string together with the Virasoro constraints and null polygonal boundary conditions on  $\partial\text{AdS}$  can be written in terms of this connection  $J$  and the flat sections that satisfy

$$(d + J(\zeta))\psi = 0, \tag{2.1}$$

where  $\zeta$  is called the spectral parameter, see [1, 7] and references therein for more details.

We will use the fact that, in a specific gauge,

$$J \underset{\zeta \rightarrow 0}{\sim} \frac{1}{\zeta} \begin{pmatrix} -\sqrt{p(z)} & 0 \\ 0 & \sqrt{p(z)} \end{pmatrix} dz \quad J \underset{\zeta \rightarrow \infty}{\sim} \zeta \begin{pmatrix} -\sqrt{\bar{p}(\bar{z})} & 0 \\ 0 & \sqrt{\bar{p}(\bar{z})} \end{pmatrix} d\bar{z} \tag{2.2}$$

where  $p(z)$  is a polynomial that encodes the shape of the polygon.

The minimal surface in terms of the embedding coordinates is encoded in  $\psi$  and can be obtained as described in [7].

### 3 Y-system

In this section we introduce the Y-system by looking at the example of the harmonic oscillator. This enables us to study the theory with a well known problem and to compare with explicit solutions. The framework is also easily extended to include all potentials of the form  $V(x) = x^{2M}$  with  $M \in \mathbb{N}$ .

The first parts regarding the two-component form of the Schrödinger equation is inspired by [8] with reference [9] while the later part follows [1]. We will here focus on the details that will be most useful to us and use slightly different methods to derive the main results of [1] – methods that are more easily extended to finding the small solutions.

Consider the time-independent, one dimensional Schrödinger equation

$$-\frac{d^2}{dx^2}\Psi(x) + V(x)\Psi(x) = E\Psi(x). \quad (3.1)$$

We note that with this normalization the eigenvalues for the harmonic oscillator  $V = x^2$  are  $E = 2n + 1$  with  $n = 0, 1, 2, \dots$

Introduce another field  $\Phi \equiv \frac{1}{Q(x)} \frac{d}{dx}\Psi$  where  $Q(x) \equiv \sqrt{V(x) - E}$ . The Schrödinger equation can now be written as a system of first order differential equations:

$$\begin{aligned} \frac{d}{dx}\Psi &= Q(x)\Phi \\ \frac{d}{dx}\Phi &= Q(x)\Psi - \frac{Q'(x)}{Q(x)}\Phi. \end{aligned} \quad (3.2)$$

We take the combinations  $\phi_{\pm} \equiv \frac{1}{2}(\Psi \pm \Phi)$  which then satisfy

$$\begin{aligned} \frac{d}{dx}\phi_+ &= \left( +Q(x) - R(x) \right)\phi_+ + R(x)\phi_- \\ \frac{d}{dx}\phi_- &= \left( -Q(x) - R(x) \right)\phi_- + R(x)\phi_+, \end{aligned} \quad (3.3)$$

where

$$R(x) \equiv \frac{1}{2} \frac{Q'(x)}{Q(x)}.$$

To simplify the differential equations and to make contact with the similar equations for the scattering amplitudes we define

$$\begin{aligned}
\psi_{\pm}(z) &\equiv -i\sqrt{2Q(x)}\phi_{\pm}(x) && \text{with } z = E^{-\frac{1}{2M}}x \\
q(z) &\equiv \sqrt{p(z)} \equiv \sqrt{z^{2M} - 1} \\
r(z) &\equiv \frac{1}{2} \frac{q'(z)}{q(z)} \\
\zeta &\equiv E^{-\frac{1+M}{2M}},
\end{aligned} \tag{3.4}$$

where we let  $z$  be a complex variable.

The polynomial  $p(z)$  corresponds to the polynomial of the scattering amplitudes discussed above. The variable  $\zeta$  will in this context be called the spectral parameter and the solutions  $\psi = (\psi_+, \psi_-)$  are called sections to relate to the scattering amplitude picture.

We obtain

$$\begin{aligned}
&(\partial_z + J)\psi = 0 \\
J &\equiv \begin{pmatrix} -\frac{1}{\zeta}\sqrt{p(z)} & -r(z) \\ -r(z) & +\frac{1}{\zeta}\sqrt{p(z)} \end{pmatrix},
\end{aligned} \tag{3.5}$$

where  $J$  is called the connection. The sections can then be formally written as

$$\psi(z) = \text{P exp} \left( - \int_{z_0}^z J(w) dw \right) \psi(z_0), \tag{3.6}$$

which can be seen as the parallel transport of  $\psi(z_0)$ .

Notice that in the limit  $\zeta \rightarrow 0$  we obtain a connection very similar to that of the scattering amplitudes in (2.2) where the spectral parameter is now essentially the energy in the Schrödinger equation. The explicit solutions are discussed in section 5.

By considering an equivalent form of the equations, in terms of Pauli matrices, we find an interesting property of the sections

$$\left( \mathbb{1}\partial_z - \sigma^1 r(z) - \sigma^3 \frac{1}{\zeta} \sqrt{p} \right) \psi = 0. \tag{3.7}$$

Since  $\sigma^1 \sigma^3 \sigma^1 = -\sigma^3$  we get that if  $\psi(\zeta; z)$  is a solution to the equations, then so is also  $\psi(e^{i\pi}\zeta; z)$ . This property will be used extensively when we analyze the solutions below.

The spectral parameter is often written on the form  $\zeta = e^\theta$  and to simplify our expressions we introduce the notation  $f^\pm(\theta) \equiv f(\theta \pm i\frac{\pi}{2})$ . For  $\zeta$  we have that  $f^\pm(\zeta) = f(e^{i\pi/2}\zeta)$  where, generally,  $f^{[4]}(\zeta) \equiv f^{++++}(\zeta) = f(e^{2\pi i}\zeta) \neq f(\zeta)$  since we typically don't identify  $\theta \approx \theta + 2\pi i$ , but instead go to another sheet. (Consider for example  $f(\zeta) = \zeta^{1/2} = e^{\theta/2}$ .)

We define an anticommuting product between two sections  $\psi_i$  and  $\psi_j$  as

$$\langle \psi_i, \psi_j \rangle = \det(\psi_i, \psi_j) = \epsilon^{\alpha\beta} (\psi_i)_\alpha (\psi_j)_\beta, \quad (3.8)$$

where the solutions are evaluated at the same  $z$ . By taking the  $z$ -derivative of the product above and using (3.5) one can show that it is independent of  $z$ .

### 3.1 Small solutions and Stokes' phenomenon

At large  $z$  we can neglect  $r(z)$  in  $J$  which goes as  $z^{-1}$ . We get an asymptotic solution

$$\begin{aligned} \psi_{\text{large } z} &\sim A_+ \underbrace{\begin{pmatrix} 1 \\ 0 \end{pmatrix} \exp \left[ +\frac{1}{\zeta} \int^z \sqrt{p(w)} dw \right]}_{\psi_+} + A_- \underbrace{\begin{pmatrix} 0 \\ 1 \end{pmatrix} \exp \left[ -\frac{1}{\zeta} \int^z \sqrt{p(w)} dw \right]}_{\psi_-} \\ &\sim A_+ \begin{pmatrix} 1 \\ 0 \end{pmatrix} \exp \left[ +\frac{1}{\zeta} \frac{z^{M+1}}{M+1} \right] + A_- \begin{pmatrix} 0 \\ 1 \end{pmatrix} \exp \left[ -\frac{1}{\zeta} \frac{z^{M+1}}{M+1} \right], \end{aligned} \quad (3.9)$$

which we will call the large- $z$  asymptote. The proportionality factors  $A_\pm$  can in general be functions of the spectral parameter  $\zeta$ .

The solutions span a two dimensional space, but it is only a specific choice of  $A_+$  and  $A_-$  that give a vanishing solution at large  $z$  in a given wedge of the complex  $z$ -plane. Such solutions will be called small solutions. We see that the choice  $A_+ = 0$  and  $A_- = 1$  gives a small solution for  $\text{Re}(z^{M+1}) > 0$  e.g.  $|\arg z| < \pi/(2M+2)$ .

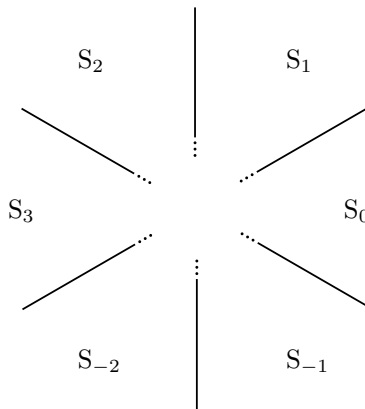


**Figure 2:** Stokes sectors in the case of  $M = 2$

We get  $2M + 2$  different sectors  $S_k$  called Stokes sectors as pictured in figure 2, each with a unique (up to normalization) exponentially decaying solution  $s_k$ . The asymptotic expansion for the small solution in sector zero with real positive  $\zeta$

$$s_0 \underset{\text{large } z}{\sim} A_0 \begin{pmatrix} 0 \\ 1 \end{pmatrix} \exp \left[ -\frac{1}{\zeta} \omega(z) \right] \quad (3.10)$$

$$\omega(z) \equiv \int^z \sqrt{p(w)} dw,$$

is valid in  $S_0$  as well as in the nearby  $S_{-1}$  and  $S_1$ . In  $S_{-1} \cup S_1$  the solution  $s_0$  is exponentially increasing because here  $\text{Re}(z^{M+1}) < 0$ . Recall though, that this is only the large  $z$  asymptote in  $S_{-1} \cup S_1$  and that there might be an exponentially decaying term hiding behind it in these regions. Thus, when we reach  $S_2$  for example,  $s_0$  is, in general, not exponentially decreasing again because of the potential, hidden term in  $S_1$  that now has become large. This behavior for the solutions is called the Stokes' phenomenon. See also figure 9 where the phenomenon is shown by the explicit solutions.

The uniqueness of the small solutions is assured by the fact that we have a two dimensional solution space which can be decomposed as in (3.9) and that a large solution can't be added to a small solution without making it large. In contrast, a large solution remains a large solution in general if we add another large or small solution.

### 3.1.1 Shift relations

We showed earlier that if  $s_0$  is a solution to (3.7), then so is also  $\sigma^1 s_0^{++}$  and we now see by smoothly changing  $\theta$  while rotating  $z$  that

$$\sigma^1 s_0^{++} \underset{\text{large } z}{\sim} B_0 \begin{pmatrix} 1 \\ 0 \end{pmatrix} \exp \left[ +\frac{1}{\zeta} \omega(z) \right] \quad (3.11)$$

is small in  $S_1$  where  $\text{Re } \omega(z) < 0$  (recall that the asymptotic expansion is valid in the neighbouring sector as well). This must be proportional to the unique small solution in  $S_1$ . From  $s_0$  we can now define small solutions in every sector by

$$s_k \equiv C^k s_0^{[2k]} \quad C \equiv i\sigma^1 \quad (3.12)$$

where  $f^{[2k]}(\theta) = f(\theta + i\pi k)$ . The extra factor of  $i$  in  $C$  have been included for the following property to hold:

$$\begin{aligned} \langle s_i, s_k \rangle^{++} &= \langle C^{-1} s_{i+1}, C^{-1} s_{k+1} \rangle = \det(C^{-1}) \det(s_{i+1}, s_{k+1}) = 1 \cdot \det(s_{i+1}, s_{k+1}) \\ &= \langle s_{i+1}, s_{k+1} \rangle \end{aligned} \quad (3.13)$$

Note for later that  $\det C = 1$  and  $C^2 = -1$ .

To simplify our expressions we will normalize  $s_0$  such that  $\langle s_0, s_1 \rangle = 1$ . Using (3.13) we then get that all  $\langle s_i, s_{i+1} \rangle = 1$ . Keep in mind though that this does not fix the normalization completely – we still have a freedom of letting  $s_0 \rightarrow f(\theta)s_0$  where  $f^+ f^- = 1$  as will be discussed later. Such a function  $f(\theta)$  will be called a zero mode in this context.

## 3.2 The Schouten identity

The Schouten identity is an identity for  $2 \times 2$  determinants or, equivalently, two-component spinors with an anticommuting product  $\langle \psi_i, \psi_j \rangle$  denoted  $\langle i, j \rangle$  for brevity.

Two linearly independent solutions  $\psi_i$  and  $\psi_j$  to (3.5) span the two-dimensional space of solutions.

Thus, a third can be written as

$$\psi_k = a\psi_i + b\psi_j, \quad (3.14)$$

where  $a$  and  $b$  are  $z$ -independent coefficients.

We now take the product with  $\psi_j$  and  $\psi_i$  on the left to get

$$\begin{aligned} a &= \frac{\langle j, k \rangle}{\langle j, i \rangle} \\ b &= \frac{\langle i, k \rangle}{\langle i, j \rangle} \end{aligned} \quad (3.15)$$

$$\langle i, j \rangle \psi_k = -\langle j, k \rangle \psi_i + \langle i, k \rangle \psi_j.$$

Multiplying with another  $\psi_l$  on the right we get the Schouten identity

$$\langle i, j \rangle \langle k, l \rangle + \langle i, l \rangle \langle j, k \rangle + \langle i, k \rangle \langle l, j \rangle = 0. \quad (3.16)$$

### 3.3 Hirota equations

We will now introduce a special case of the Hirota equations. These types of functional equations are typically encountered when studying integrable models where the involved functions, in that case, are eigenvalues of transfer matrices [1].

Let us define the  $T$ -functions as

$$\begin{aligned} T_{2k+1} &= \langle s_{-k-1}, s_{k+1} \rangle \\ T_{2k} &= \langle s_{-k-1}, s_k \rangle^+ . \end{aligned} \quad (3.17)$$

Outside of the range  $s = 0, \dots, n-2$ , where  $n$  is the number of small solutions, we let  $T_s$  be zero as done in [1].

Using the Schouten identity (3.16) and our normalization  $\langle s_i, s_{i+1} \rangle = 1$  we get the Hirota equations

$$T_s^+ T_s^- = T_{s-1} T_{s+1} + 1. \quad (3.18)$$

### 3.4 Y-system equations

Specific to our choice of normalization, we define the  $Y$ -functions as

$$Y_s = T_{s-1}T_{s+1}, \quad (3.19)$$

Since  $Y_s$  is the product of two next-to-nearest neighbouring  $T$ -functions we have that  $Y_s$  is nonzero only for  $s = 1, \dots, n - 3$  [1].

Using our definitions (3.17) this can be written more explicitly as

$$\begin{aligned} Y_{2k} &= \langle s_{-k}, s_k \rangle \langle s_{-k-1}, s_{k+1} \rangle \\ Y_{2k+1} &= \langle s_{-k-1}, s_k \rangle^+ \langle s_{-k-2}, s_{k+1} \rangle^+. \end{aligned} \quad (3.20)$$

In [1] they give a more general form of the  $Y$ -functions and show that they are independent on the choice of normalization – where we use  $\langle i, i + 1 \rangle = 1$  as mentioned above. The  $Y$ -functions are physical objects with a geometrical description described below.

Using the Hirota equation on  $Y_s^+ Y_s^-$  written as  $T$ -functions we get the  $Y$ -system equations

$$Y_s^+ Y_s^- = (1 + Y_{s+1})(1 + Y_{s-1}). \quad (3.21)$$

These relations are essentially rewritten Schouten identities without real physical content. The physical input that is required comes from the asymptotics which we will obtain in the following section.

### 3.5 Geometrical interpretation

To get a geometrical picture of the  $Y$ -functions we will consider a normalization independent definition from [1]

$$\begin{aligned}
 Y_{2k} &= \frac{\langle s_{-k}, s_k \rangle \langle s_{-k-1}, s_{k+1} \rangle}{\langle s_{-k-1}, s_{-k} \rangle \langle s_k, s_{k+1} \rangle} \\
 Y_{2k+1} &= \left( \frac{\langle s_{-k-1}, s_k \rangle \langle s_{-k-2}, s_{k+1} \rangle}{\langle s_{-k-2}, s_{-k-1} \rangle \langle s_k, s_{k+1} \rangle} \right)^+.
 \end{aligned} \tag{3.22}$$

Notice that, using the normalization  $\langle s_i, s_{i+1} \rangle = 1$ , we retrieve (3.20).

We are interested in the geometrical interpretation of the  $Y$ -functions in the limit when  $\theta \rightarrow -\infty$ . For the scattering amplitudes, we will see that both limits  $\theta \rightarrow \pm\infty$  work in a similar way.

#### 3.5.1 WKB limit

Let us now introduce the main tool for finding the asymptotic behavior of the  $Y$ -functions. For a more rigorous treatment in a related case see [10, Appendix C].

We need a way to describe the products  $\langle s_i, s_j \rangle$  above as  $\theta \rightarrow -\infty$ . Such a product can be understood by transporting  $s_i$  in sector  $i$  to  $s_j$  in sector  $j$  using the connection  $J(z)$  as described above<sup>1</sup>

$$s_i(w') = \text{P exp} \left( - \int_w^{w'} J(z) dz \right) s_i(w). \tag{3.23}$$

Say that we asymptotically know each solution  $s_k$  in a neighbourhood around the point  $z_k$  – for example at large  $z_k$  in sector  $k$  using the large- $z$  asymptote (3.9) as illustrated in figure 3. We will now use the fact that  $J$  becomes diagonal as  $\zeta \rightarrow 0$ , which we will call the WKB limit, to transport the small solution.

Some care has to be taken though in how we apply this to the asymptotic expression for  $s_i$ . We have to keep track of the initial asymptotics such that we don't enlarge a sub-leading term. For this reason, let us consider the example of transporting  $s_0$  starting from  $z_0$ .

---

<sup>1</sup>Repeated here for convenience in a slightly different notation

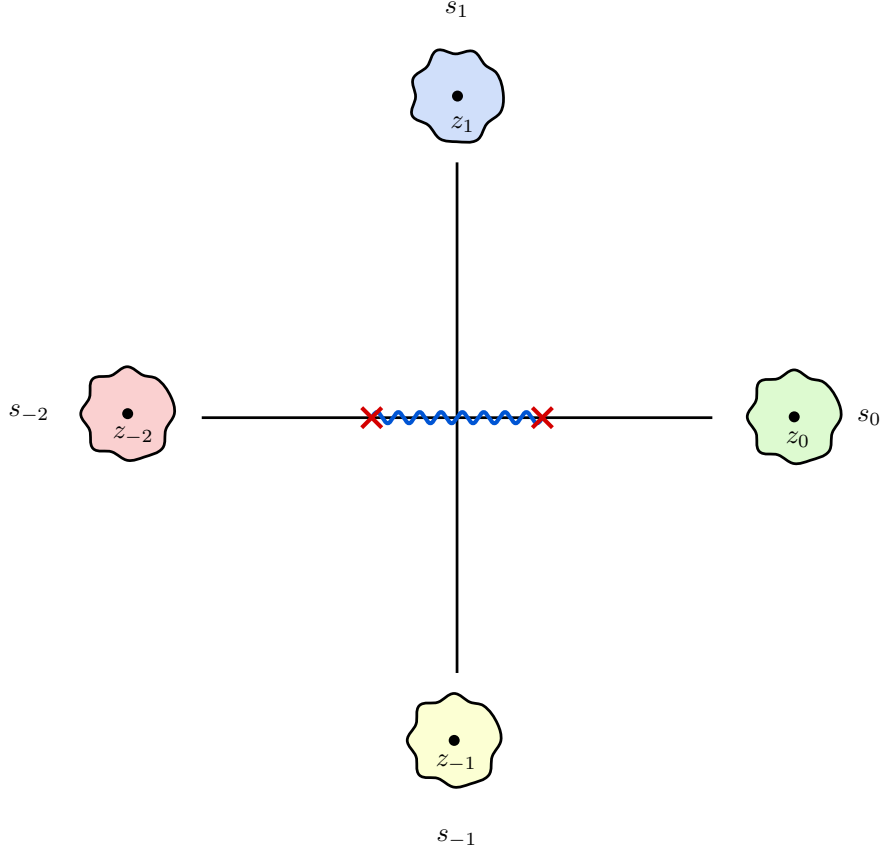


**Figure 3:** Small solutions for the harmonic oscillator and the octagon with roots (red) and branch-cut (blue) of  $p(z)$ . We imagine that the small solution  $s_i$  is known in a neighbourhood around  $z_i$ .

For large  $z_0$  in sector zero we know that

$$s_0(z_0) \underset{\text{large } z_0}{\sim} A_0 \begin{pmatrix} 0 \\ 1 \end{pmatrix} \exp\left(-\frac{1}{\zeta} \int^{z_0} \sqrt{p(z)} dz\right) \quad (3.24)$$

and in the WKB limit

$$-J dz \underset{\zeta \rightarrow 0}{\sim} \begin{pmatrix} \frac{1}{\zeta} \sqrt{p} dz & 0 \\ 0 & -\frac{1}{\zeta} \sqrt{p} dz \end{pmatrix} \quad (3.25)$$

When applying this to  $s_0(z_0)$  above we want the factor  $\exp\left(-\frac{1}{\zeta} \sqrt{p} dz\right)$  to strengthen the leading

asymptote which is done when  $\operatorname{Re}\left(-\frac{1}{\zeta}\sqrt{p}dz\right) > 0$ . It becomes the most strengthening when  $\operatorname{Im}\left(\frac{1}{\zeta}\sqrt{p}dz\right) = 0$  which gives us a direction  $dz$  where we can safely parallel transport the small solution. The lines these differentials form are called WKB lines.

For the small solution  $s_1(z_1)$  we instead have

$$s_1(z_1) \underset{\text{large } z_1}{\sim} A_1 \begin{pmatrix} 1 \\ 0 \end{pmatrix} \exp\left(+\frac{1}{\zeta} \int^{z_1} \sqrt{p(z)} dz\right) \quad (3.26)$$

for which we require the other eigenvalue of  $J$  to become strengthening, i.e.  $\operatorname{Re}\left(+\frac{1}{\zeta}\sqrt{p}dz\right) > 0$ , but still  $\operatorname{Im}\left(\frac{1}{\zeta}\sqrt{p}dz\right) = 0$ . The WKB lines are the same for both types of small solutions, but the directions vary.

We see that if we follow this strict direction of the steepest ascent, every point  $z$  (besides the roots of  $p$ ) can flow only along one WKB line and in one direction. To be able to catch and arrive by different WKB lines we use the fact that we know the asymptotic expansion of the small solution  $s_k$  in a *neighbourhood* around  $z_k$  as shown in figure 3.

Note that even though we let  $\zeta \rightarrow 0$  we still have some choice in which direction, i.e. the argument of  $\zeta$ . This enables us to adjust the WKB lines to some degree which will (hopefully) be enough for the products considered in the  $Y$ -functions above. In fact, it is shown in [1] that setting the phase of  $\zeta$  to  $e^{i\pi/4}$  is enough for all the products we use.

### 3.5.2 Branch cuts

An important situation is when the WKB lines approaches a branch cut of  $\sqrt{p(z)}$ . Let us discuss that in a bit more detail.

Instead of only using the complex plane for  $z$  we imagine that we live on a Riemann surface obtained by analytically continuing  $\sqrt{p}$  as seen in figure 4 in the case of the harmonic oscillator.

When traveling along a WKB line, we follow the analytical continuation of  $\sqrt{p}$  and thus walking smoothly along the Riemann surface. While doing numerical calculations though, we work with single valued functions and have to choose one sheet of the surface by introducing branch cuts. At

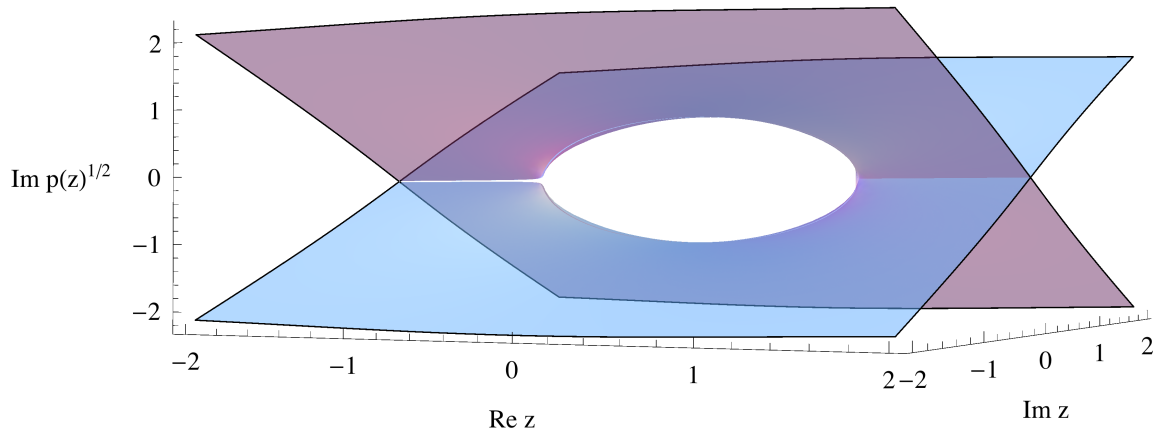


**Figure 4:** The Riemann surface of  $\text{Im} \sqrt{p(z)}$  where  $p(z) = z^2 - 1$ .

these branch cuts the single valued function becomes discontinuous which we have to account for by going to the next sheet when doing the WKB lines.

### 3.5.3 Harmonic oscillator and octagon

We are now ready to discuss the geometrical interpretation of the  $Y$ -functions. Let us concentrate on the case of  $Y_1$  with a second degree polynomial  $p(z)$  that is positive for large real  $z$  and has real roots. This is the case both for the harmonic oscillator and for the octagon in the scattering amplitude picture.

The WKB lines can be seen in figure 5. Note that the arrows denote the direction of steepest ascent for the solutions that are initially defined at the arrow tail. The other solution must be transported in the opposite direction.

From the normalization independent definition we have that

$$Y_1 = \left( \frac{\langle s_{-1}, s_0 \rangle \langle s_{-2}, s_1 \rangle}{\langle s_{-2}, s_{-1} \rangle \langle s_0, s_1 \rangle} \right)^+. \quad (3.27)$$

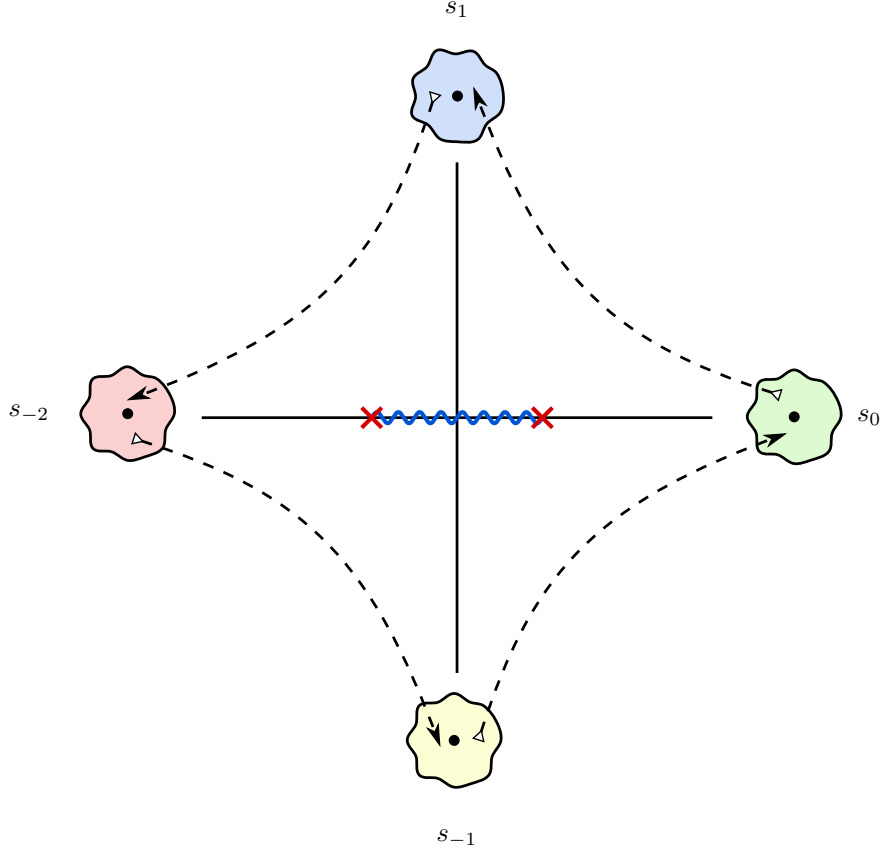


**Figure 5:** WKB lines for the harmonic oscillator and the octagon. The directions are for the solutions where the arrow starts.

We take a closer look at the product  $\langle s_0, s_1 \rangle$  where

$$s_0(z_1) \underset{\zeta \rightarrow 0}{\sim} \exp\left(-\frac{1}{\zeta} \int_{z_0}^{z_1} \sqrt{p} dz\right) s_0(z_0), \quad (3.28)$$

which gives

$$\langle s_0, s_1 \rangle \underset{\zeta \rightarrow 0}{\sim} \exp\left(-\frac{1}{\zeta} \int_{z_0}^{z_1} \sqrt{p} dz\right) \det\left(s_0(z_0), s_1(z_1)\right). \quad (3.29)$$

The same is done with the other products forming  $Y_1$ , being careful to only follow the WKB lines.

Note that, when calculating the determinants, we get each component both in the numerator

and the denominator. Thus, the  $s_k(z_k)$  components cancel, which shows that the  $Y$ -function is normalization independent and we obtain

$$\log Y_1 \underset{\zeta \rightarrow 0}{\sim} \left( \frac{1}{\zeta} \oint_{\gamma_1} \sqrt{p} dz \right)^+ = \frac{1}{i\zeta} \oint_{\gamma_1} \sqrt{p} dz, \quad (3.30)$$

with  $\gamma_1 : z_{-1} \rightarrow z_0 \rightarrow z_1 \rightarrow z_{-2} \rightarrow z_{-1}$  which we can deform to a simple contour running around the roots counter clockwise. In the case of the harmonic oscillator where  $p(z) = z^2 - 1$  we get that  $\log Y_1 \underset{\zeta \rightarrow 0}{\sim} -\pi/\zeta$ .

The asymptotics for all the  $Y$ -functions can be related to such cycles of  $\sqrt{p}$ , sometimes entering both sheets. The contours and all pre-factors can be found in [1].<sup>2</sup>

For the scattering amplitudes, we see from (2.2) that the limit  $\zeta \rightarrow \infty$  works in a similar way, but now taking cycles of  $\sqrt{p}$  which can be shown to be the same as those above for polynomials with roots on the real line [1].

### 3.6 Y-system integral equations

By looking at the geometrical interpretation of the  $Y$ -functions we have now probed their asymptotic behavior. Let us summarize some of the results from above in terms of  $\theta$  where  $\zeta = e^\theta$ .

For the Schrödinger problem we have that  $\log Y_s \sim -m_s e^{-\theta}$  as  $\theta \rightarrow -\infty$  where  $m_s$  comes from the cycles of  $\sqrt{p(z)}$  and can be shown to be real and positive in the case of polynomials with real roots [1]. In the other limit we see that the  $\theta$ -dependence in the differential equation (3.5) for  $\psi$  drops out, which means that the only  $\theta$  dependence of the small solutions in this limit comes from the normalization. This leads us to the conclusion that  $Y_s$  goes to a constant as  $\theta \rightarrow \infty$  since it is constructed to be independent of normalization and  $z$ .

In the case of the scattering amplitudes we have similar asymptotic expansions in both limits with  $\log Y_s \sim -\frac{1}{2}m_s e^{-\theta}$  as  $\theta \rightarrow -\infty$  and  $\log Y_s \sim -\frac{1}{2}m_s e^\theta$  as  $\theta \rightarrow +\infty$  with the same, positive  $m_s$ .

---

<sup>2</sup>Note that there is a factor of two relating the definition of  $m_s$  in this paper compared to the case of the Schrödinger problem.

*Summa summarum*,  $Y_s \sim \exp[-Z_{Y_s}(\theta)]$  for large  $|\theta|$  up to constant pre-factors where

$$Z_{Y_s}(\theta) = \begin{cases} m_s e^{-\theta} & \text{for Schrödinger} \\ m_s \cosh \theta & \text{for scattering amplitudes} \end{cases} \quad (3.31)$$

We don't need to worry about the extra constants of proportionality since the following arguments only rely on the fact that  $\tilde{Y}_s \equiv Y_s / \exp(-Z_{Y_s})$  is bounded as  $\theta \rightarrow \pm\infty$  [11].

Note that  $Z_{Y_s}^+ = -Z_{Y_s}^-$  for both cases. From (3.21) we then get that

$$\tilde{Y}_s^+ \tilde{Y}_s^- = Y_s^+ Y_s^- = (1 + Y_{s+1})(1 + Y_{s-1}), \quad (3.32)$$

or, equivalently with  $l_s \equiv \log \tilde{Y}_s$

$$l_s^+ + l_s^- = \log \left( (1 + Y_{s+1})(1 + Y_{s-1}) \right). \quad (3.33)$$

By design,  $l_s$  is bounded (and in the case of the scattering amplitudes it goes to zero in both limits of  $\theta$ ). This means that we can use an  $\epsilon$ -regularized Fourier transform to solve the above equation for  $l_s$  [11].

Denoting  $\hat{l}_s(\omega) = \mathcal{F}[l_s(\theta)](\omega) = \int_{-\infty}^{\infty} l_s(\theta) e^{-i\omega\theta} d\theta$  we find that  $\mathcal{F}[l_s^\pm](\omega) = e^{\mp\omega\pi/2} \hat{l}_s(\omega)$  where it is assumed that we don't pass any poles of  $l_s$  when shifting the contour with  $\text{Im } \theta : \pm\pi/2 \rightarrow 0$ . Thus,

$$2 \cosh \frac{\pi\omega}{2} \hat{l}_s = \mathcal{F} \left[ \log \left( (1 + Y_{s+1})(1 + Y_{s-1}) \right) \right]. \quad (3.34)$$

Inverting this we find  $l_s$  as the convolution

$$l_s = K_Y \star \log \left( (1 + Y_{s+1})(1 + Y_{s-1}) \right) \quad (3.35)$$

$$K_Y(\theta) = \mathcal{F}^{-1} \left[ \frac{1}{2 \cosh \frac{\pi\omega}{2}} \right](\theta) = \frac{1}{2\pi \cosh \theta}$$

Hence, we get that

$$\log Y_s(\theta) = -Z_{Y_s}(\theta) + \int_{-\infty}^{\infty} d\theta' K_Y(\theta - \theta') \log \left( (1 + Y_{s+1}(\theta'))(1 + Y_{s-1}(\theta')) \right), \quad (3.36)$$

which is one of the results of [1].

We note that when  $\text{Im } \theta$  approaches  $\pm\pi/2$  we hit a pole in the kernel. Since we assume that the  $Y$ -functions are analytic, the expression (3.36) can only be true for  $|\text{Im } \theta| < \pi/2$ . Beyond that we would either have to pick up a residue from the kernel (as explained further in the section for the  $T_1$  function below) or simply use (3.21) to recursively find an expression in terms of  $Y$ -functions inside this strip of validity.

The integral equations enables us to solve for the  $Y$ -functions iteratively by first inserting the asymptotic expressions for all  $Y_s$  in (3.36) with a convergence that is very fast.

Another important note is that, for the harmonic oscillator and the octagon, we have only one  $Y$ -function which is then completely given by its asymptote as seen in (3.36). The constant pre-factor is obtained from (3.21) which gives  $Y_1 = \exp(-Z_{Y_1})$ .

Finally, using the  $Y$ -functions the regularized area can be computed by

$$A = \sum_s \int d\theta \frac{m_s}{2\pi} \cosh \theta \log (1 + Y_s(\theta)), \quad (3.37)$$

as explained in [1].

## 4 Finding the small solutions

Before we can solve for the small solutions we need to find  $T_1$  numerically in terms of the  $Y$ -functions that we found an expression for above. The method is very similar; we will use the functional relation (3.19) between  $T$ 's and  $Y$ 's, find the large  $|\theta|$  asymptotes for  $T_1$  and write an integral expression using Fourier analysis. Since  $T_1$  is normalization dependent we first need to discuss the normalization of the small solutions.

## 4.1 Normalization

Using the shift relation (3.12) we can obtain all the small solutions from  $s_0$  and normalizing  $s_0$  such that  $\langle s_0, s_1 \rangle = 1$  results in  $\langle s_i, s_{i+1} \rangle = 1$  for all  $i$  as discussed above. But as we also covered, there is some freedom left in choosing the normalization, namely  $s_0 \rightarrow s'_0 = f(\theta)s_0$  where  $f$  is a zero mode  $f^+f^- = 1$  which still leaves  $\langle s_0, s_1 \rangle = 1$ .

The remaining freedom in normalization gives us the possibility of changing the behavior of  $T_1$  as

$$T'_1 \equiv \langle s'_{-1}, s'_1 \rangle = f^{--}f^{++}\langle s_{-1}, s_1 \rangle = f^{--}f^{++}T_1 = \frac{T_1}{f^2}, \quad (4.1)$$

where we, in the last step, have used that  $f$  is a zero mode.

From the Hirota equations we have that (since  $m_1$  is positive)

$$T_1^+T_1^- = 1 + Y_1 \underset{\theta \rightarrow -\infty}{\sim} 1 + e^{-m_1 e^{-\theta}} \underset{\theta \rightarrow -\infty}{\sim} 1. \quad (4.2)$$

Thus,  $T_1$  is asymptotically a zero mode and have the expansion  $T_1 \sim e^{g(\theta)}$  as  $\theta \rightarrow -\infty$  where  $g^+ + g^- = 0$ . We can then choose  $f(\theta) = e^{\frac{1}{2}g(\theta)}$  so that  $T'_1 \rightarrow 1$  as  $\theta \rightarrow -\infty$  and  $f^+f^- = 1$ .

After renormalizing  $s_0$  such that  $T_1 \sim 1$  as  $\theta \rightarrow -\infty$  one can argue that the small solutions have asymptotic expansions of the form

$$s_0 \underset{\theta \rightarrow -\infty}{\sim} A_0 \begin{pmatrix} 0 \\ 1 \end{pmatrix} \exp \left[ -\frac{1}{\zeta} \left( \int^z \sqrt{p} + B_0 \right) \right] \quad (4.3)$$

where  $A_0$  and  $B_0$  are constants with respect to both  $\zeta$  and  $z$ . This is consistent with  $s_0$  satisfying (3.5) in the WKB limit where  $J$  becomes diagonal but adding the additional statement that the normalization only enters as an integration constant  $B_0$  and an overall, constant, factor  $A_0$ .

By comparing with the explicit solutions for the harmonic oscillator in this normalization we found that this is indeed the case and could determine  $A_0$  and  $B_0$ .

The argument is similar for the scattering amplitudes where  $Y_1 \rightarrow 1$  in both limits, but here the non-renormalized  $T_1$  could in general have two different zero modes as asymptotic expansions in

the two limits  $\theta \rightarrow \pm\infty$ . There is strong evidence, though, for that they can be dealt with using the same  $f$ .<sup>3</sup>

The limit  $\theta \rightarrow \infty$  is a bit special in the case of the harmonic oscillator where we have allowed ourselves to depend more on the explicit solutions. We see that the  $\theta$  dependence drops out from the connection in this limit and the small solutions can then be found as

$$s_0 = D(\theta) \begin{pmatrix} -1 \\ 1 \end{pmatrix} \frac{1}{(z^2 - 1)^{\frac{1}{4}}}, \quad (4.4)$$

where  $D(\theta)$  is a normalization factor.

Using the prescription for renormalizing  $T_1$  in the other limit above we find from the explicit expressions that

$$D(\theta) = \frac{(-1)^{\frac{1}{4}} \sqrt{\pi}}{\Gamma(\frac{1}{4})} e^{\theta/4} \quad (4.5)$$

This behavior makes  $T_1$  go to a constant in the  $\theta \rightarrow \infty$  limit and since  $Y_1 \rightarrow 1$  as  $\theta \rightarrow \infty$  this constant has to be  $\sqrt{2}$  from combining (3.18) and (3.19) which gives

$$T_s^+ T_s^- = 1 + Y_s \quad (4.6)$$

## 4.2 Integral equation for $T_1$

The functional relation between  $T_1$  and  $Y_1$  we need is directly given by (4.6).

We found above that  $T_1$  goes to a constant in both limits  $\theta \rightarrow \pm\infty$  for both the scattering amplitudes and the harmonic oscillator. That  $T_1$  is bounded means that we can use the Fourier transform to invert the relation above after taking the logarithm of both sides. We find that

$$\begin{aligned} \log T_1 &= K_T \star \log(1 + Y_1) \\ K_T(\theta) &= K_Y(\theta) = \frac{1}{2\pi \cosh \theta} \end{aligned} \quad (4.7)$$

---

<sup>3</sup>Even if this should be proven not to be the case the integral equations for  $T_1$  are easily modified to include any zero mode asymptotics as was done for the  $Y$ -functions.

Finally,

$$\log T_1(\theta) = \int_{-\infty}^{\infty} d\theta' K_T(\theta - \theta') \log(1 + Y_1(\theta')). \quad (4.8)$$

Indeed, we now see that for the harmonic oscillator  $T_1 \rightarrow \sqrt{2}$  when  $\theta \rightarrow \infty$  as expected since, for large  $\theta$ , the convolution picks up a contribution only at large  $\theta'$  because of the kernels compact support. As  $\theta' \rightarrow \infty$  we have that  $\log(1 + Y_1(\theta')) \sim \log 2$ . The integral can then be written as  $\int_{-\infty}^{\infty} d\theta' (2\pi \cosh \theta')^{-1} \log 2 = (1/2) \log 2$ .

### 4.2.1 Picking up residues

We see that the integral equation (4.8) is also only valid for  $|\text{Im } \theta| < \pi/2$  since the kernel  $K_T(\theta - \theta')$  has the same form as for the  $Y$ -functions and has poles at  $\theta - \theta' = i\pi/2 + i\pi k$  with  $k \in \mathbb{Z}$ . We assume that  $T_1$  is analytic and will now discuss how to go beyond this strip of validity.

The picture we should have in mind is the following. The integration variable  $\theta'$  follows the contour that is the real line and when smoothly changing  $\text{Im } \theta$  we move the poles as seen in the  $\theta'$  plane.

Our integral expression (4.8) is still valid when translating the poles or shifting the contour of integration as long as the all the poles above the contour stays above the contour and similarly for the ones below as can be seen from Cauchy's integral theorem.

If a pole tries to sneak over the contour in either direction when changing  $\text{Im } \theta$  we have to cancel its contribution by either adding or removing the residue as illustrated in figure 6.

When increasing  $\text{Im } \theta$  above  $\pi/2$  new poles cross the contour from below which are canceled by removing their residues (times  $2\pi i$ ) on the right hand side of the integral equation. Decreasing  $\text{Im } \theta$  below  $-\pi/2$  instead makes poles cross from above which we cancel by adding their residues.

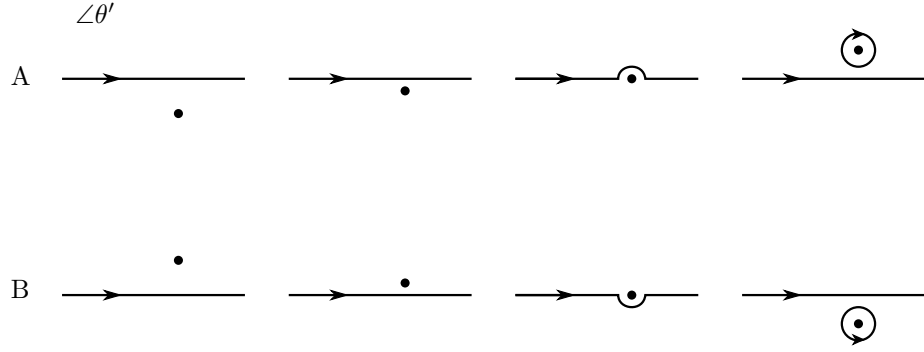


**Figure 6:** Cancellations of poles (dots) crossing the integration contour in the  $\theta'$  plane

The residues at  $\theta' = \alpha_k \equiv \theta - i\pi/2 - i\pi k$  of the kernel together with an analytic function  $f(\theta')$  are found as

$$\begin{aligned}
\oint_{\gamma_k} \frac{1}{2\pi \cosh(\theta - \theta')} f(\theta') d\theta' &= \left\{ \theta' = \alpha_k + \epsilon \right\} = \oint_{\gamma_0} \frac{1}{2\pi \cosh(i\frac{\pi}{2} + i\pi k - \epsilon)} f(\alpha_k + \epsilon) d\epsilon \\
&= \oint_{\gamma_0} \frac{(-1)^{k+1}}{2\pi i \sinh \epsilon} f(\alpha_k + \epsilon) d\epsilon = \oint_{\gamma_0} \frac{(-1)^{k+1}}{2\pi i \epsilon} f(\alpha_k + \epsilon) + \dots d\epsilon = (-1)^{k+1} f(\alpha_k),
\end{aligned} \tag{4.9}$$

where  $\gamma_k$  are positively oriented, closed contours around  $\alpha_k$  and  $\gamma_0$  is the equivalent around the origin.

Thus, if we let  $\bar{T}_1(\theta)$  be defined as in (4.8) without picking up poles as we shift  $\theta$  we get that

$$\log T_1(\theta) = \begin{cases} \log \bar{T}_1(\theta) & -\frac{\pi}{2} < \text{Im } \theta < \frac{\pi}{2} \\ -(-1)^{0+1} \log \left( 1 + Y_1(\theta - i\frac{\pi}{2}) \right) + \log \bar{T}_1(\theta) & \frac{\pi}{2} < \text{Im } \theta < \frac{3\pi}{2} & k = 0 \\ -(-1)^{1+1} \log \left( 1 + Y_1(\theta - i\frac{3\pi}{2}) \right) + \\ -(-1)^{0+1} \log \left( 1 + Y_1(\theta - i\frac{\pi}{2}) \right) + \log \bar{T}_1(\theta) & \frac{3\pi}{2} < \text{Im } \theta < \frac{5\pi}{2} & k = 1, 0 \end{cases} \tag{4.10}$$

where the first minus signs are needed because the residues should be removed in this direction (A in figure 6). When going in the other direction we would instead add the residues for negative  $k$  (B in the same figure).

### 4.3 Integral equation for the small solutions

To numerically solve for the small solutions we will use the fact that the space of all solutions is two dimensional. Thus, by taking products with  $s_{-1}$  and  $s_1$  again using the notation  $\langle i, j \rangle \equiv \langle s_i, s_j \rangle$  we get (compare with the derivation of (3.16))

$$s_0 = as_{-1} + bs_1 \tag{4.11}$$

$$a = \frac{\langle 0, 1 \rangle}{\langle -1, 1 \rangle} \quad b = \frac{\langle -1, 0 \rangle}{\langle -1, 1 \rangle}$$

which in our normalization ( $\langle i, i+1 \rangle = 1$ ) becomes

$$T_1 s_0 = \langle -1, 1 \rangle s_0 = s_{-1} + s_1 = C^{-1} s_0^{--} + C s_0^{++} = C(s_0^{++} - s_0^{--}), \tag{4.12}$$

or, equivalently,

$$CT_1 s_0 = s_0^{--} - s_0^{++} \tag{4.13}$$

We now have a functional relation for the small solution  $s_0$  and would like to use the asymptotes of  $s_0$  to define a quantity that is bounded in both limits. We would then be able to use Fourier analysis to invert the expression above and find an integral equation in a similar way as for the  $Y$ -functions and  $T_1$

In the normalization section above we argued for the asymptotic behavior of  $s_0$  with some normalization issues sorted out using the explicit solutions in appendix A.

We found that in sector zero

$$s_0 \underset{\theta \rightarrow -\infty}{\sim} V_L \exp(-Z_{s_0}(\theta, z)) \quad s_0 \underset{\theta \rightarrow \infty}{\sim} V_R \exp(\theta/4) \tag{4.14}$$

$$Z_{s_0}(\theta, z) = e^{-\theta} \left( \int^z \sqrt{p(w)} dw + \text{const.} \right)$$

$$V_L = (-1)^{\frac{1}{4}} \begin{pmatrix} 0 \\ 1 \end{pmatrix} \quad V_R = \frac{(-1)^{\frac{1}{4}} \sqrt{\pi}}{(z^2 - 1)^{\frac{1}{4}} \Gamma(\frac{1}{4})} \begin{pmatrix} -1 \\ 1 \end{pmatrix}$$

Let us define

$$\tilde{s}_0 \equiv \frac{s_0 - V_L \exp(-Z_{s_0}(\theta, z))}{\exp(-Z_{s_0}(\theta, z)) \exp(\theta/4)}, \quad (4.15)$$

which has the properties (for  $z \in S_0$ )

$$\begin{aligned} \tilde{s}_0 &\rightarrow 0 \text{ as } \theta \rightarrow -\infty \quad \text{because the correction to the WKB wins over } \exp(\theta/4) \\ \tilde{s}_0 &\rightarrow V_R \text{ as } \theta \rightarrow \infty \end{aligned} \quad (4.16)$$

Since  $Z_{s_0}^{\pm\pm} = -Z_{s_0}$  we get that

$$\begin{aligned} s_0 &= e^{-Z_{s_0}} (\tilde{s}_0 e^{\theta/4} + V_L) \\ s_0^{\pm\pm} &= e^{+Z_{s_0}} (\tilde{s}_0^{\pm\pm} e^{\pm i\pi/4} e^{\theta/4} + V_L), \end{aligned} \quad (4.17)$$

which modifies (4.13) to

$$e^{-i\pi/4} \tilde{s}_0^{--} - e^{i\pi/4} \tilde{s}_0^{++} = CT_1 e^{-2Z_{s_0}} (\tilde{s}_0 + V_L e^{-\theta/4}) \quad (4.18)$$

As before, we invert this relation using Fourier analysis and find the integral equation

$$\begin{aligned} \tilde{s}_0 &= C K_{s_0} \star T_1 e^{-2Z_{s_0}} (\tilde{s}_0 + V_L e^{-\theta/4}) \\ K_{s_0}(\theta) &= \mathcal{F}^{-1} \left[ \frac{1}{2 \sinh \pi(\omega - i/4)} \right] (\theta) = \frac{i e^{\theta/4}}{4\pi \cosh(\theta/2)} \quad (z \in S_0). \end{aligned} \quad (4.19)$$

$\tilde{s}_0$  can now be found iteratively by first inserting a smooth function with the correct limits from (4.16). The small solution  $s_0$  can then be obtained using (4.17).

Note that the integral expression can only be valid in the strip  $-\pi < \text{Im } \theta < \pi$  after which we pick up poles from the kernel.

Also note that in the case of the scattering amplitudes we expect more symmetric asymptotic expansions of the small solutions as argued above – the  $\theta \rightarrow \infty$  limit being different for the harmonic oscillator. Asymptotic expansions of the WKB form in both limits (as is expected for the scattering amplitudes) simplifies the kernel above, but the general method stays the same.

### 4.3.1 Other sectors

Above, we explained how to numerically find  $s_0$  in  $S_0$ . Let us now first generalize to finding the small solution  $s_k$  in  $S_k$  which proves to be easier than the next case of computing the small solution outside its own sector. The latter we will do for the case of  $s_0$  in  $S_1$  and  $S_2$  which are easily generalized.

#### $s_k$ in $S_k$

We will start from (4.19) and use the shift relations. This requires some care in making sure we pick up all necessary residues and that we keep the  $e^{-2Z_{s_0}}$  factor suppressing so that the integral converges. While discussing how the poles crosses the contour we will imagine that  $k$  is positive but the same arguments can be made for negative  $k$ .

Increasing  $\theta$  for  $\tilde{s}_0$  in (4.19) moves the poles in the  $\theta'$  plane upwards and we need to remove the residues as in figure 6 (A). Let us introduce the shorthand notation

$$h(\theta') \equiv T_1(\theta')e^{-2Z_{s_0}(\theta')}(\tilde{s}_0(\theta') + V_L e^{-\theta'/4}), \quad (4.20)$$

where we suppress the  $z$ -dependence of  $h$ .

Thus,

$$\begin{aligned} \tilde{s}_0(\theta) &= C \int_{-\infty}^{\infty} d\theta' K_{s_0}(\theta - \theta') h(\theta') \\ \tilde{s}_0^{[2k]}(\theta) &\equiv \tilde{s}_0(\theta + i\pi k) = C \int_{-\infty}^{\infty} d\theta' K_{s_0}(\theta - \theta' + i\pi k) h(\theta') - (\text{residues}). \end{aligned} \quad (4.21)$$

We make a simple change of variables  $\theta'' = \theta' - i\pi k$ , without deforming the contour.

$$\tilde{s}_0^{[2k]}(\theta) = C \int_{-\infty - i\pi k}^{\infty - i\pi k} d\theta'' K_{s_0}(\theta - \theta'') h^{[2k]}(\theta'') - (\text{residues}). \quad (4.22)$$

When now shifting the contour to the real axis again we will sweep over the same poles that got introduced earlier and will now be added with the opposite sign – canceling all the residues. Imagine

figure 6 (B) with the pole stationary while the contour moves upwards.

The result is then

$$\tilde{s}_0^{[2k]}(\theta) = C \int_{-\infty}^{\infty} d\theta'' K_{s_0}(\theta - \theta'') h^{[2k]}(\theta'') \quad (z \in S_k). \quad (4.23)$$

We note that the factor  $\exp(-2Z_{s_0}(\theta', z))$  is now suppressing for  $z \in S_k$ .

All the small solutions  $s_k$  can now be found iteratively for  $z \in S_k$  in the same way as for  $s_0$  in  $S_0$ .

### $s_0$ in $S_1$

When going outside sector zero the factor  $\exp(-2Z_{s_0}(\theta', z))$  makes the integral in (4.19) diverging. As  $z$  moves continuously across the complex plane counter clockwise we need to shift the contour accordingly, but first we will start with a simple change of variables  $\theta'' = \theta' - i\pi$

$$\tilde{s}_0(\theta) = C \int_{-\infty - i\pi}^{\infty - i\pi} d\theta'' K_{s_0}^{[-2]}(\theta - \theta'') h^{[2]}(\theta'') \quad (4.24)$$

The kernel  $K_{s_0}^{[-2]}(\theta - \theta'')$  has poles at  $\theta'' = \theta + 2i\pi n$ . Assuming  $\theta \in \mathbb{R}$ , we will meet the pole at  $\theta'' = \theta$  as we shift the contour to the real line. Note that we can't let the contour run straight over the pole but we have to go around it in the lower half plane as shown in figure 7. This is equal to taking the Cauchy principal value and half the residue.

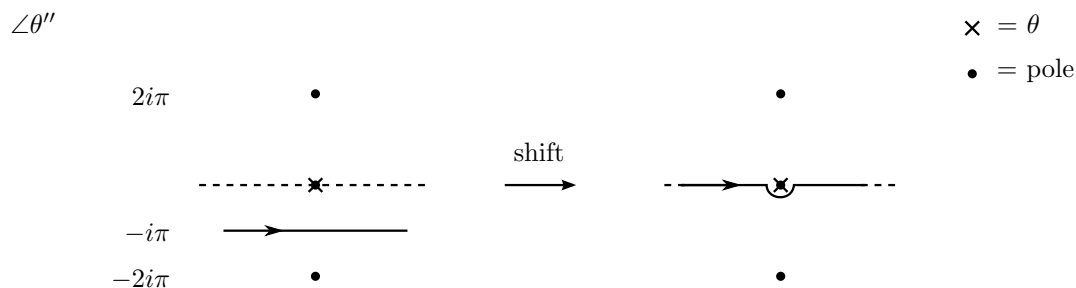


**Figure 7:** Deformation of the contour as we avoid the pole on the real line.

We expand the kernel around  $\theta'' = \theta$  and find that  $K_{s_0}^{[-2]}(\theta - \theta'') = \frac{e^{i\frac{\pi}{4}}}{2i\pi(\theta'' - \theta)} + \dots$  which gives

$$\tilde{s}_0(\theta) = C \left( \frac{e^{i\frac{\pi}{4}}}{2} h^{[2]}(\theta) + \int_{-\infty}^{\infty} d\theta'' K_{s_0}^{[-2]}(\theta - \theta'') h^{[2]}(\theta'') \right) \quad (z \in S_1). \quad (4.25)$$

Notice that the right hand side contains  $\tilde{s}_0^{++}$  in  $S_1$  which is essentially  $s_1$  in  $S_1$  that can be computed using (4.23). The small solutions  $s_0$  can then be found directly by integration without resorting to further iterations. We can in this way find all  $s_k$  in  $S_{k+1}$  and, similarly, in  $S_{k-1}$ .

### $s_0$ in $S_2$

Let us continue from (4.25) to the next sector  $S_2$  by first making a change of variables without changing the contour

$$\begin{aligned} \tilde{s}_0(\theta) &= C \left( \frac{e^{i\frac{\pi}{4}}}{2} h^{[2]}(\theta) + \int_{-\infty}^{\infty} d\theta' K_{s_0}^{[-2]}(\theta - \theta') h^{[2]}(\theta') \right) \\ &= \left\{ \theta'' = \theta - i\pi \right\} = \\ &= C \left( \frac{e^{i\frac{\pi}{4}}}{2} h^{[2]}(\theta) + \int_{-\infty - i\pi}^{\infty - i\pi} d\theta'' K_{s_0}^{[-4]}(\theta - \theta'') h^{[4]}(\theta'') \right). \end{aligned} \quad (4.26)$$

When shifting the contour to make the exponential suppressing we will now completely envelope the pole we previously only partially encircled. More rigorously,  $K_{s_0}^{[-4]}(\theta - \theta'')$  has poles at  $\theta'' = \theta + i\pi + 2i\pi n$  and our initial  $\theta''$ -contour above goes slightly under the pole  $\theta - i\pi$  where we still imagine  $\theta \in \mathbb{R}$ . When shifting  $\theta''$  to the real line we will circle the pole once and should, besides the integral, have the complete residue of this pole as well. See figure 8.

This is exactly the result we would have obtained by starting from (4.19) and shifting the contour by  $2\pi i$  at once, completely enveloping the pole. Since the pole is no longer on the contour along the real line, the Cauchy principal value is not necessary.

Finally,

$$\tilde{s}_0(\theta) = C \left( e^{i\frac{\pi}{4}} h^{[2]}(\theta) + \int_{-\infty}^{\infty} d\theta'' K_{s_0}^{[-4]}(\theta - \theta'') h^{[4]}(\theta'') \right) \quad (z \in S_2). \quad (4.27)$$

Here, the right hand side depends on  $s_1$  in  $S_2$  and  $s_2$  in  $S_2$  which can be found using the two

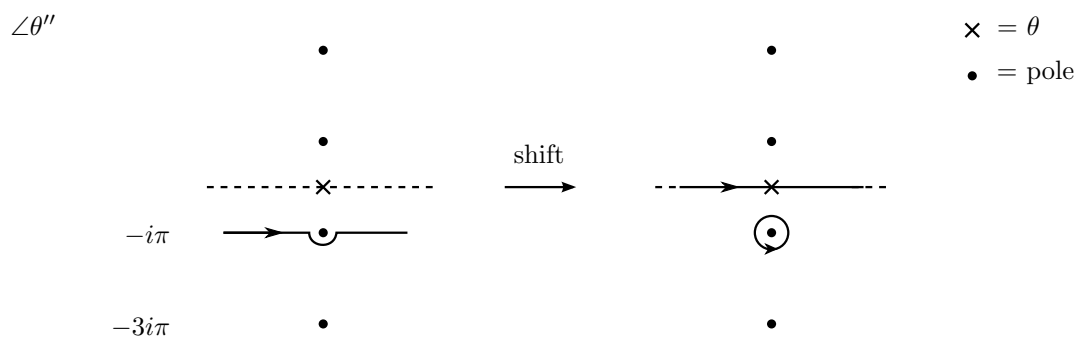


**Figure 8:** Further shifting of the contour to envelope the whole pole.

previous methods above. As before,  $s_0$  in  $S_2$  is then obtained by direct integration. With these results we can easily extend a small solution  $s_k$  to a general sector  $S_m$ .

## 5 The harmonic oscillator

After developing these methods for finding the small solutions, let us now apply them to the harmonic oscillator and compare with the known solutions.

The explicit solutions were obtained by solving (3.1) with  $V(x) = x^2$  for all energies using Mathematica. Without the conditions that the solution should be bounded in both sector  $S_0$  and  $S_2$ <sup>4</sup> we get a continuous spectrum in the energy  $\zeta^{-1}$  with solutions written in terms of parabolic cylinder functions. These are then written in a two-component form according to (3.4).

We obtain a two dimensional space of solutions and choose the direction that have a vanishing solution at large  $z$  in  $S_0$ . This will be our  $s_0$ . The normalization is found by first requiring that  $\langle s_0, s_1 \rangle = 1$  and then by fixing  $T_1 \sim 1$  as  $\theta \rightarrow -\infty$  as described in section 4.1. The final expressions for  $s_0$  and  $T_1$  are included in appendix A.

From these expressions we notice that the small solutions express the Stokes' phenomenon in figure 9 as expected and at the physical energy  $E = 1$ , i.e.  $\theta = 0$  we see that  $s_0$  is small in both  $S_0$  and  $S_2$ .

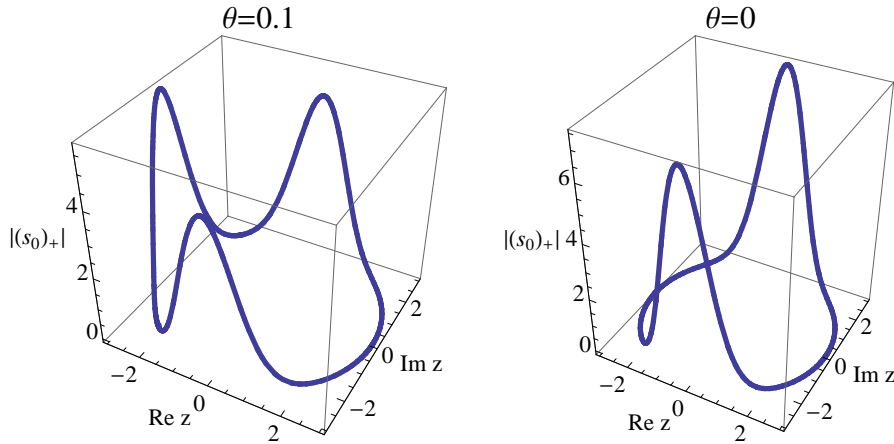


**Figure 9:** The absolute value of the first component of  $s_0$  as  $z = 3\exp(i\varphi)$ ,  $\varphi : 0 \rightarrow 2\pi$ . We notice the Stokes' phenomenon for the small solutions and that, at the physical energy corresponding to  $\theta = 0$ ,  $s_0$  is small in both  $S_0$  and  $S_2$ .

<sup>4</sup>When solving for physical wave functions one usually imposes that they vanish as  $x \rightarrow \pm\infty$ .

The  $Y$ -system for the harmonic oscillator is trivial since  $Y_1$  is given by its asymptotic expansion. We integrate around the roots of  $p(z)$  as implied by figure 5 to find  $m_1 = \pi$  and thus  $Y_1 = \exp(-\pi e^{-\theta})$ . From this we can use (4.10) with generalization to find  $T_1$ . In figure 10 we compare the numerical computations with the explicit  $T_1$  obtained from  $T_1 = \langle s_{-1}, s_1 \rangle$  and find complete agreement. Note that without the inclusion of residues,  $T_1$  would be periodic with  $T_1(\theta) = T_1(\theta + 2\pi i)$  and discontinuous as in figure 11.

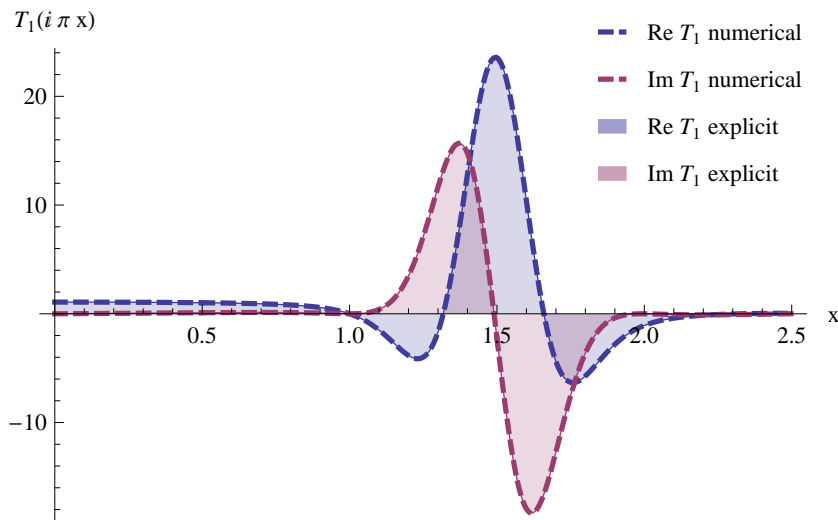


**Figure 10:** Comparison between numerical  $T_1$  from (4.10) and explicit expression

To test the integral equations for  $s_0$  in  $S_0$ ,  $S_1$  and  $S_2$  from (4.19, 4.25, 4.27) we insert the explicit solution, which should solve the equation, on the right hand side of the equation and compare with the same solution on the left hand side. The result for one specific value of  $z$  in each sector is shown in figure 12 where the expressions are found to match perfectly.

Now that we have verified the integral equations we can start solving for  $s_0$  in  $S_0$  iteratively using the integral equation (4.19). As a starting position for the iterations we use

$$\tilde{s}_0 = \frac{e^\theta}{1 + e^\theta} V_R, \quad (5.1)$$

where  $V_R$  is defined in (4.14) and which has the proper behavior of (4.16).

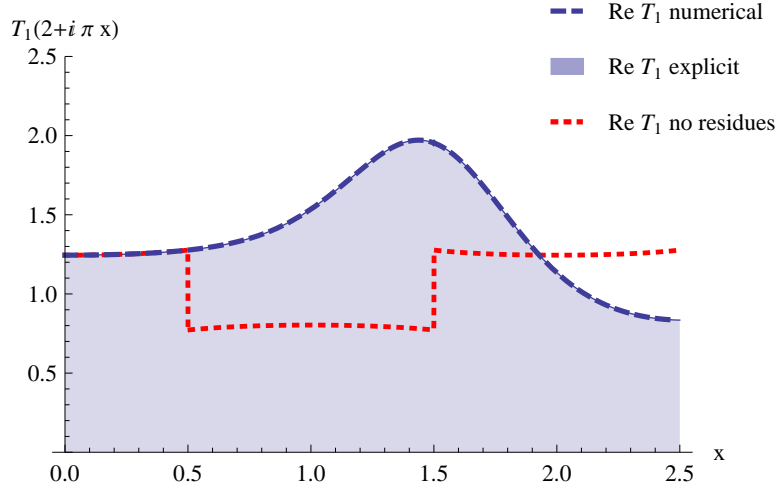


**Figure 11:** Illustration of  $T_1$  with and without extra residues together with explicit solution

The results for the three first iterations at the point  $z = 3.14 + 0.5i$  can be seen in figure 14 which are already quite good. We note the strange fact that the second component seems to get worse between the second and the third iteration. Also, it seems like, at each iteration, one component is better than the other and that which component this is alternates between iterations.

Taking a closer look with more iterations one sees that this is indeed the case as is also shown in figure 13 (left) where we study the difference between the numerical and explicit solutions. The two components alternate but both are ultimately converging. From the combined errors of the two components in figure 13 (right) we see that the total deviation is decreasing monotonically.

When computing the numerical solutions one would benefit from taking advantage of this behavior. If one has computed the small solutions to the eight iteration as in figure 13, one could in this case use component 1 from iteration 7 while taking component 2 from iteration 8.

We have noticed that the convergence is fast (a few iterations) for all but very large, positive  $\theta$ . In figure 14 we include a frame where we have gone as far as to 30 iterations. The iterative solution converges perfectly to the explicit solution.

All included, the methods developed in the previous sections have been proven very successful and we would now like to extend them to the case of the scattering amplitudes.

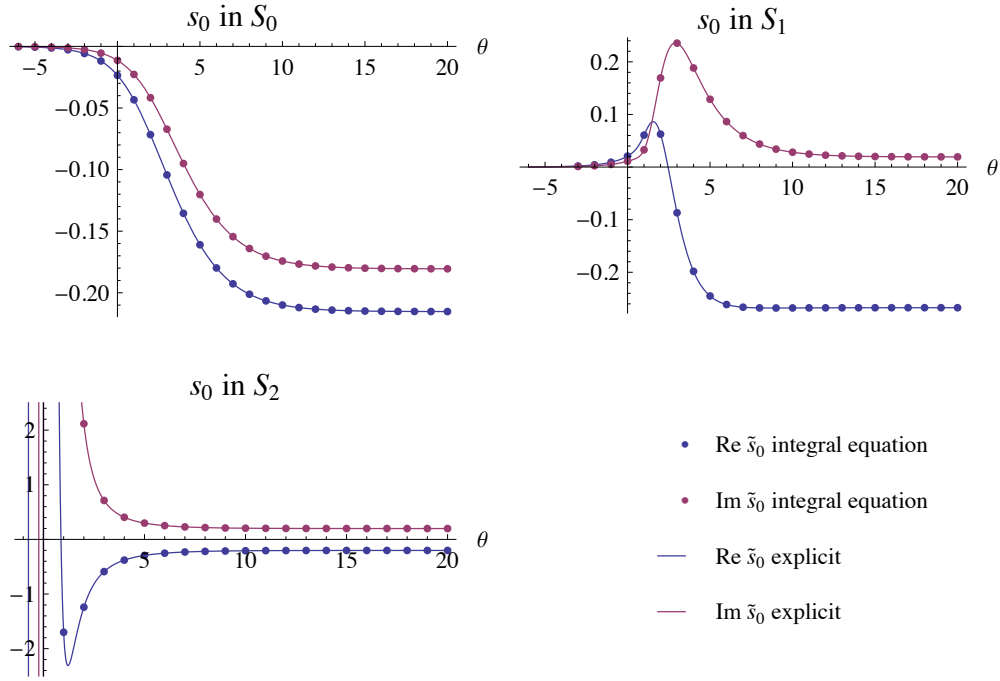


**Figure 12:** We insert the explicit solution in the integral equations above and see that we retrieve the small solution again. Here we show the first component at one specific value of  $z$  in each sector.

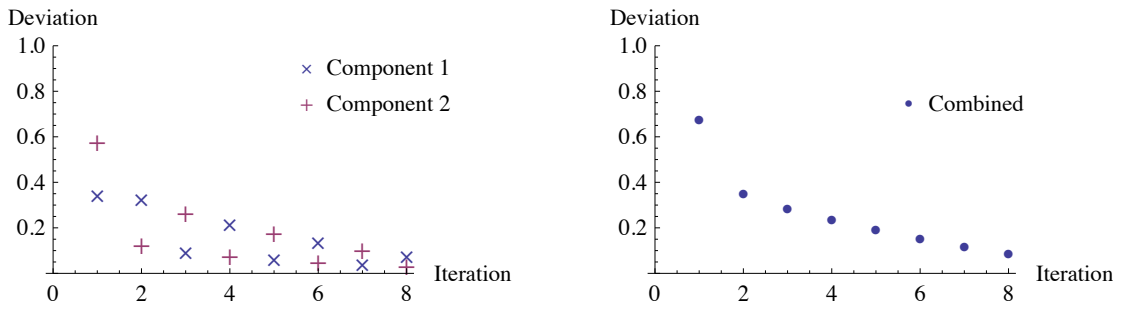


**Figure 13:** The convergence of  $\tilde{s}_0$  from figure 14. The deviation  $\Delta_\alpha$  for component  $\alpha$  (left) is defined by  $\Delta_\alpha^2 = \int ((\tilde{s}_0 \text{ numerical})_\alpha - (\tilde{s}_0 \text{ explicit})_\alpha)^2 d\theta$ . The combined deviation  $\Delta$  (right) is defined by  $\Delta^2 = \Delta_1^2 + \Delta_2^2$ .

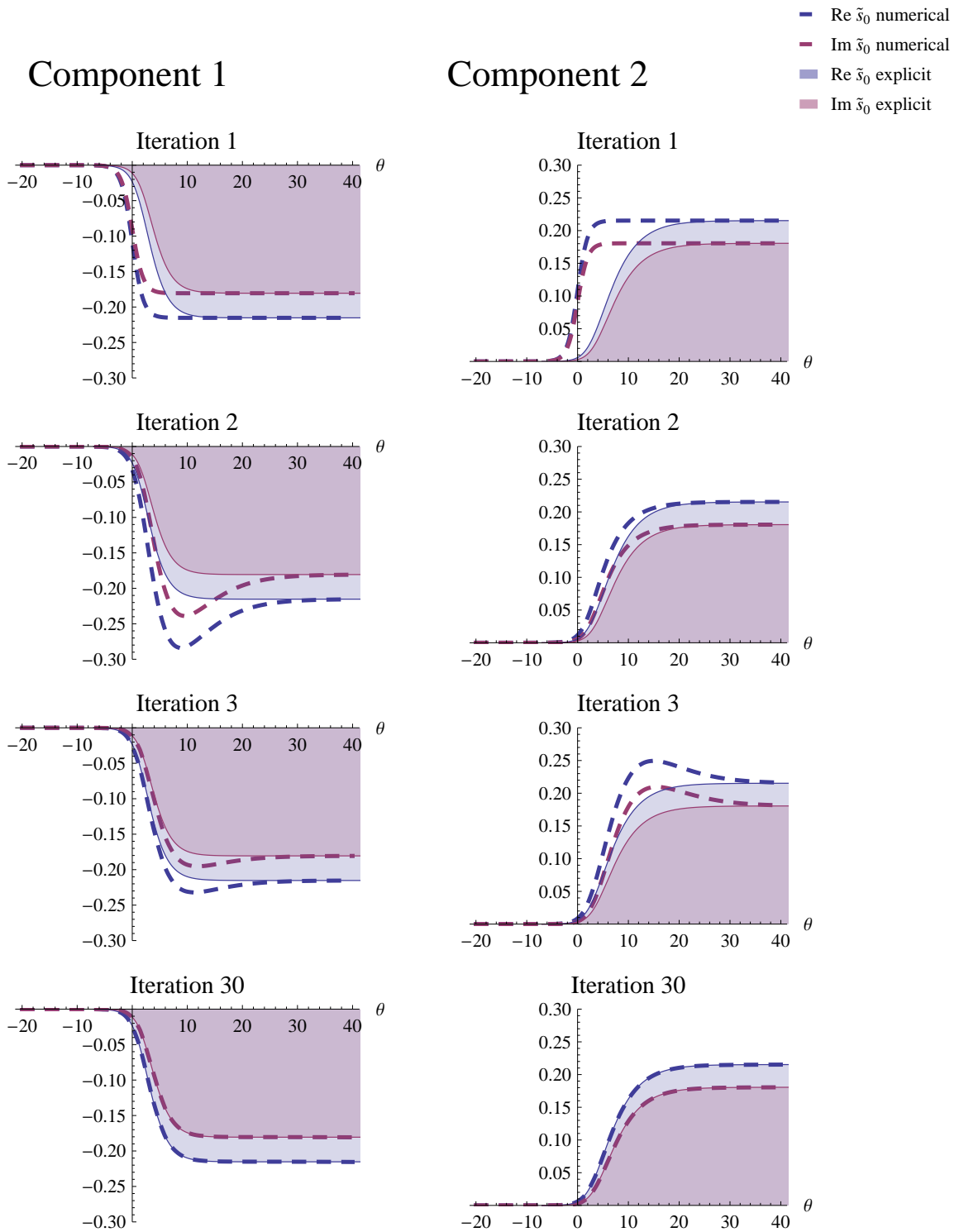


**Figure 14:** Iteratively solving for  $\tilde{s}_0$  at  $z = 3.14 + 0.5i$ . Note that the components alternate at being the best fitting component between iterations.

## 6 Scattering amplitudes

The equations for the small solutions in the scattering amplitudes case are very similar to those of the harmonic oscillator. We can directly translate most of the results, especially those regarding the limit  $\theta \rightarrow -\infty$ .

In the other limit the two problems differ, but the scattering amplitudes are usually easier to deal with since their  $\theta \rightarrow \infty$  limit is very similar to  $\theta \rightarrow -\infty$ .

Thus, the asymptotic expansions that were used to make, for example,  $\tilde{s}_0$  bounded change, and in fact, the new expression should now only contain zero modes as was the case in  $\theta \rightarrow -\infty$ . This greatly simplifies (4.17) and therefore also the kernel  $K_{s_0}$  together with the factor it is convoluted with. Most other functional relations are still valid provided that we update the asymptotic expansions.

Future developments involve studying the normalization and behavior of  $T_1$  in both limits and apply the methods above to the scattering amplitudes. Ultimately, we want to find the small solutions for the scattering amplitudes in all sectors and use these to find the minimal surface in  $\text{AdS}_3$  as described in [7, Section 2.2]. An illustration of such a surface can be found in figure 1.

## 7 Conclusions

In this essay we have developed a method for finding the small solutions in the two-component formalism of the harmonic oscillator. This was shown to be very similar to the problem of finding the minimal surface of a string world sheet in  $\text{AdS}_3$  ending on a null polygon on the border of  $\text{AdS}$ .

We have briefly introduced the one parameter family of flat connections and the corresponding equations for the flat sections which would give us the minimal surface. We derived a two-component equation starting from the Schrödinger equation and pointed out the resemblance to the flat sections.

Using the example of the Schrödinger equation we defined the small solutions, discussed the Stokes' phenomenon and obtained the  $Y$ -system equations. After that we found the asymptotic expansion of the  $Y$ -functions and obtained their geometrical interpretation.

The  $Y$ -system equations were written as integral equations that could be solved iteratively and similar integral equations were found for  $T_1$  and the small solutions after discussing the issue of normalization. We showed how shifting  $\theta$  introduced extra residues to our integral expressions and how the small solutions  $s_k$  are computed in any sector  $S_m$ .

Next, the methods were tested by applying them to the two-component harmonic oscillator where the solutions are already explicitly known. We found that they were very successful and that the convergence was fast.

Finally, we discussed how this can be applied to the minimal surfaces for scattering amplitudes and future developments.

## Acknowledgements

I would like to give my sincere gratitude to my supervisor Pedro Vieira and his PhD student Jonathan Toledo for all their support, inspiration and encouragement.

Thank you Pedro for all your help and guidance! I has been a great pleasure to work with you and I have learned so much these months. I owe it all to you.

Jon, thank you for all your time, detailed explanations and for your well written essay that helped me a lot. What would I have done without you?

Also, thank you Amit Sever for all your useful insights and for the Mathematica notebook used to generate figure 1.

Last, but not least, thanks to all my dear classmates, family and friends for their endless support and understanding.

## A Explicit expressions

From the procedure explained in section 5 we got the explicit solutions for the two component harmonic oscillator as

$$s_0 = \frac{(-1)^{\frac{1}{4}} 2^{\frac{1}{4}} (e^{-\theta} - 1)^{-\frac{1}{2}} e^{\frac{1}{4}e^{-\theta}(\theta+1) - \frac{\theta}{4}}}{(z^2 - 1)^{\frac{1}{4}}} \begin{pmatrix} (\sqrt{z^2 - 1} + z)D_{\nu_1}(\omega) - \sqrt{2}e^{\theta/2}D_{\nu_2}(\omega) \\ (\sqrt{z^2 - 1} - z)D_{\nu_1}(\omega) + \sqrt{2}e^{\theta/2}D_{\nu_2}(\omega) \end{pmatrix} \quad (\text{A.1})$$

where  $\omega = \sqrt{2}e^{-\theta/2}z$ ,  $\nu_1 = \frac{1}{2}(e^{-\theta} - 1)$ ,  $\nu_2 = \frac{1}{2}(e^{-\theta} + 1)$  and  $D_\nu$  are the parabolic cylinder functions.

The renormalized  $T_1$  is then found as

$$T_1 = \frac{\pi 2^{1-e^{-\theta}} e^{-\frac{1}{2}e^{-\theta}(\theta+1)}}{\Gamma\left(\frac{1}{4}(1 + e^{-\theta})\right) \Gamma\left(\frac{1}{4}(3 + e^{-\theta})\right)} \quad (\text{A.2})$$

## References

- [1] L. F. Alday, J. Maldacena, A. Sever, and P. Vieira, “Y-system for Scattering Amplitudes,” [arXiv.org:1002.2459](https://arxiv.org/abs/1002.2459) [hep-th].
- [2] N. Beisert, C. Ahn, L. F. Alday, Z. Bajnok, J. M. Drummond, L. Freyhult, N. Gromov, R. A. Janik, V. Kazakov, T. Klose, G. P. Korchemsky, C. Kristjansen, M. Magro, T. McLoughlin, J. A. Minahan, R. I. Nepomechie, A. Rej, R. Roiban, S. Schafer-Nameki, C. Sieg, M. Staudacher, A. Torrielli, A. A. Tseytlin, P. Vieira, D. Volin, and K. Zoubos, “Review of AdS/CFT Integrability: An Overview,” [arXiv:1012.3982](https://arxiv.org/abs/1012.3982) [hep-th].
- [3] J. Maldacena, “Wilson Loops in Large N Field Theories,” *Physical Review Letters* **80** no. 22, (June, 1998) 4859–4862, [arXiv:hep-th/9803002](https://arxiv.org/abs/hep-th/9803002).
- [4] L. F. Alday and R. Roiban, “Scattering Amplitudes, Wilson Loops and the String/Gauge Theory Correspondence,” [arXiv.org:0807.1889](https://arxiv.org/abs/0807.1889) [hep-th].
- [5] L. F. Alday and J. Maldacena, “Gluon scattering amplitudes at strong coupling,” [arXiv.org:0705.0303](https://arxiv.org/abs/0705.0303) [hep-th].
- [6] I. Bena, J. Polchinski, and R. Roiban, “Hidden Symmetries of the  $\text{AdS}_5 \times S^5$  Superstring,” [arXiv.org:hep-th/0305116](https://arxiv.org/abs/hep-th/0305116).
- [7] L. F. Alday and J. Maldacena, “Null polygonal Wilson loops and minimal surfaces in Anti-de-Sitter space,” [arXiv.org:0904.0663](https://arxiv.org/abs/0904.0663) [hep-th].
- [8] J. C. Toledo, “PSI Essay: Review of the ODE-IM Correspondence and Prospects for the  $O(4)$  Sigma Model,” June, 2010.
- [9] M. V. Berry and K. Mount, “Semiclassical approximations in wave mechanics,” *Rept.Prog.Phys.* **35** (1972) 315.
- [10] D. Gaiotto, G. W. Moore, and A. Neitzke, “Wall-crossing, Hitchin Systems, and the WKB Approximation,” [arXiv.org:0907.3987](https://arxiv.org/abs/0907.3987) [hep-th].
- [11] P. Dorey, C. Dunning, and R. Tateo, “The ODE/IM Correspondence,” tech. rep., Mar., 2007. [arXiv.org:hep-th/0703066](https://arxiv.org/abs/hep-th/0703066).